JBC ACCELERATED COMMUNICATION

Molecular mechanism of intramolecular electron transfer in dimeric sulfite oxidase

Received for publication, September 8, 2021, and in revised form, January 26, 2022 Published, Papers in Press, February 2, 2022,
https://doi.org/10.1016/j.jbc.2022.101668

Malin Eh[1], **Alexander Tobias Kaczmarek**[1], **Guenter Schwarz**[1,*], **and Daniel Bender**[1,2,*]

From the [1]*Department of Chemistry, Institute of Biochemistry, University of Cologne, Cologne, Germany;* [2]*Department of Pediatric Neurology, University Children's Hospital Zurich, Zurich, Switzerland*

Edited by F. Peter Guengerich

Sulfite oxidase (SOX) is a homodimeric molybdoheme enzyme that oxidizes sulfite to sulfate at the molybdenum center. Following substrate oxidation, molybdenum is reduced and subsequently regenerated by two sequential electron transfers (ETs) *via* heme to cytochrome *c*. SOX harbors both metals in spatially separated domains within each subunit, suggesting that domain movement is necessary to allow intramolecular ET. To address whether one subunit in a SOX dimer is sufficient for catalysis, we produced heterodimeric SOX variants with abolished sulfite oxidation by replacing the molybdenum-coordinating and essential cysteine in the active site. To further elucidate whether electrons can bifurcate between subunits, we truncated one or both subunits by deleting the heme domain. We generated three SOX heterodimers: (i) SOX/Mo with two active molybdenum centers but one deleted heme domain, (ii) SOX/Mo_C264S with one unmodified and one inactive subunit, and (iii) SOX_C264S/Mo harboring a functional molybdenum center on one subunit and a heme domain on the other subunit. Steady-state kinetics showed 50% SOX activity for the SOX/Mo and SOX/Mo_C264S heterodimers, whereas SOX_C264S/Mo activity was reduced by two orders of magnitude. Rapid reaction kinetics monitoring revealed comparable ET rates in SOX/Mo, SOX/Mo_C264S, and SOX/SOX, whereas in SOX_C264S/Mo, ET was strongly compromised. We also combined a functional SOX Mo domain with an inactive full-length SOX R217W variant and demonstrated interdimer ET that resembled SOX_C264S/Mo activity. Collectively, our results indicate that one functional subunit in SOX is sufficient for catalysis and that electrons derived from either $Mo^{(IV)}$ or $Mo^{(V)}$ follow this path.

Sulfite oxidase (SOX) is a homodimeric enzyme localized to the intermembrane space of mitochondria (1). In mitochondria, the enzyme oxidizes sulfite to form sulfate as the final step of cysteine catabolism (2, 3). SOX harbors two metal cofactors: a b_5-type heme and the molybdenum cofactor (Moco) (4, 5). Both cofactors are spatially separated by two different domains within each SOX subunit (6, 7) (Fig. 1*A*). The N-terminal heme domain is connected to the catalytic Moco domain by a flexible tether of 11 residues followed by a C-terminal domain responsible for homodimerization of two SOX subunits.

Within the Moco domain of SOX, the catalytic molybdenum atom is placed in the center of a square-based pyramid where it coordinates five atomic ligands (5, 8, 9). Three of these ligands are sulfur atoms, of which two are derived from a dithiolate moiety of the Moco scaffold. The third sulfur derives from a highly conserved cysteine residue within the SOX polypeptide chain (human Cys264) (10). The remaining two ligands are oxygen atoms, of which one is coordinated axially in respect to the molybdenum atom, whereas the second oxygen atom points toward the active site of SOX. The latter represents the reactive oxoligand that is used for oxotransfer to form sulfate from sulfite (11). Upon oxotransfer, the abstracted oxoligand is replaced by oxygen coordination of a water molecule, which reduces the oxidation state of the molybdenum atom from $Mo^{(VI)}$ to $Mo^{(IV)}$ (12). This defines the reductive half reaction of SOX.

The $Mo^{(VI)}$ state of SOX is regenerated in a process that includes two sequential intramolecular electron transfer (IET) reactions from molybdenum to the iron of the heme cofactor and from there to the final electron acceptor cytochrome *c* (13, 14). This is referred to as the oxidative half reaction of SOX. In between the first and second IET reaction of the enzyme, the molybdenum temporarily resides in a paramagnetic $Mo^{(V)}$ state (15). In the chicken SOX X-ray crystal structure, the metals of both cofactors are 32 Å apart, which represent an interatom distance being too large for efficient IET (6) (Fig. 1*A*). Therefore, a closed conformation of the enzyme was proposed that enables fast IET from molybdenum to iron followed by an open conformation that allows the subsequent release of the electron from the heme iron toward cytochrome *c* (16, 17). While oxidation of sulfite and the concomitant reduction of molybdenum in the reductive half reaction of SOX were measured with 541 s^{-1}, the first IET from $Mo^{(IV)}$ to the heme iron was substantially slower with rates of 80 s^{-1} at pH 7.7 and 28 s^{-1} at pH 8.0 (18, 19). The rates for the second IET within SOX revealed ET rates of up to 700 s^{-1} from $Mo^{(V)}$ to the iron of heme (20).

Loss of SOX activity leads to severe neurological symptoms, including seizures, and cumulates in early childhood death. A

* For correspondence: Guenter Schwarz, gschwarz@uni-koeln.de; Daniel Bender, daniel.bender@kispi.uzh.ch.

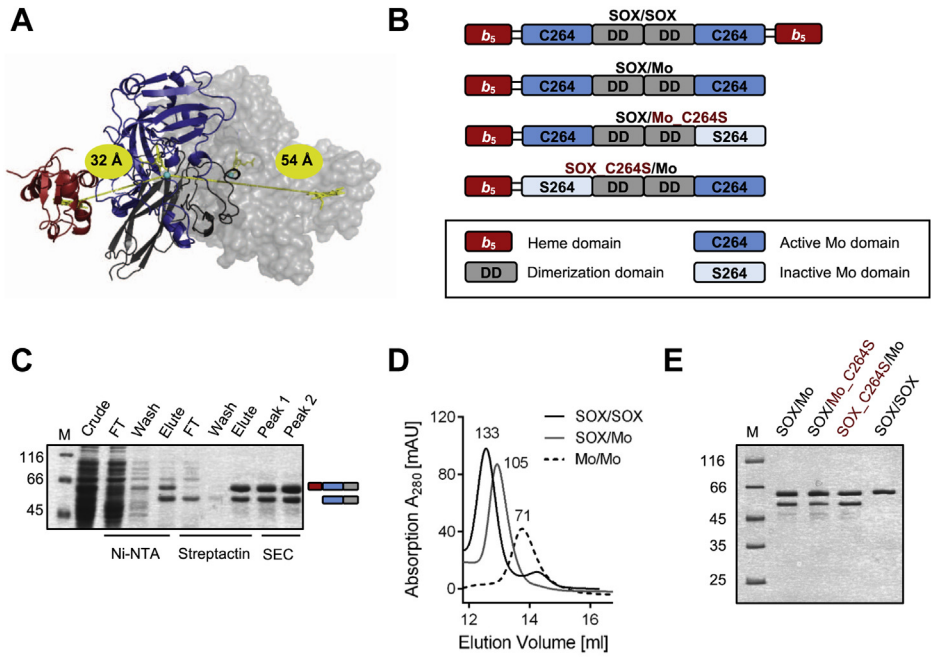

Figure 1. Purification of heterodimeric SOX. *A*, moco-to-heme distances in the crystal structure of chicken SOX. The crystal structure of chicken SOX has been previously determined by Kisker *et al.* and is available in the Protein Data Bank (ID: 1SOX). One subunit is shown in *cartoon* representation with the heme domain in *red*, the Mo domain in *blue*, and the dimerization domain in *gray*. The other subunit is shown in transparent surface representation. The Moco and heme cofactors are shown in *yellow*, and the Mo atom is shown in *cyan*. The Mo-to-Fe distances within one subunit and between two opposing subunits are 32 and 54 Å, respectively. *B*, heterodimers consist of one full-length and one truncated Mo subunit. The C264S substitution abolishes sulfite-oxidizing activity. *C*, Coomassie brilliant blue staining of a 12% SDS-PAGE containing samples collected during purification following sequential nickel–nitrilotriacetic acid, Strep-Tactin affinity chromatography, as well as preparative size-exclusion chromatography (SEC). *D*, analytical SEC of homodimeric WT SOX/SOX, heterodimeric SOX/Mo, and homodimeric Mo domain. Calculated molecular weights are shown in kilodalton. *E*, Coomassie brilliant blue staining after 12% SDS-PAGE. Per lane 2 μg or 1 μg were loaded for the heterodimeric variants and homodimeric SOX/SOX, respectively. SOX, sulfite oxidase.

deficiency in SOX can be caused by a mutation of *SUOX*, the gene that encodes the SOX enzyme, or a mutation in one of the genes required for the synthesis of Moco (21). The resulting conditions are termed isolated SOX deficiency (ISOD) or Moco deficiency, respectively. Up to date, there are 58 patients reported in the literature, carrying loss-of-function, protein truncating, and missense mutations within *SUOX* (22, 23). Amongst those, eight disease-causing missense mutations localize to the dimerization domain. Four were identified in ISOD patients, of which the G530D variant was biochemically analyzed, and its monomeric state was confirmed (24, 25). The remaining four SOX variants found in the dimerization domain were identified among naturally occurring *SUOX* mutations in a machine learning approach *in silico*, which were proven kinetically inactive *in vitro* (23). These findings suggest a functional requirement of dimer formation in SOX. Moreover, all other eukaryotic Moco-dependent enzymes, except for the mitochondrial amidoxime–reducing component, are homodimeric enzymes in which each subunit is equipped with enzyme-specific cofactors (26).

Using SOX as the prototype of Moco-dependent enzymes, we asked whether one active subunit in a dimer is sufficient for catalytic sulfite oxidation (27). As dimerization is critical for SOX catalysis, we tempted to keep dimerization behavior intact by deleting catalytic functionality of only one subunit in a SOX dimer. With this tool, we asked whether SOX adopts a conformation in which IET occurs between molybdenum and iron of opposing subunits and whether this is the functional need of SOX dimerization. Therefore, a sequential purification method was established with which it was possible to purify recombinantly expressed human SOX (hSOX) as heterodimeric protein. These SOX heterodimers consisted of a full-length (FL) subunit and a truncated subunit that lacked the N-terminal heme domain (Fig. 1*B*). By replacing the molybdenum-coordinating cysteine 264 to serine on either side of a heterodimer, we abolished sulfite reactivity (10) in the truncated or FL subunit, thereby generating SOX heterodimers with controlled electron flow. We revealed the IET-competent conformation to be limited to a single subunit, thereby excluding electron bifurcation in a SOX dimer. Furthermore, by using a combination of different SOX variants, we clarify the complex pathway of electron flow constituting two fast ET steps within a SOX dimer followed by two slow intermolecular ET steps.

Results

Purification of heterodimeric SOX variants

In order to investigate whether ET from molybdenum to heme in SOX takes place as intrasubunit ET or in an intersubunit trans-pathway from one subunit to the other, we generated heterodimeric SOX variants and compared them with WT SOX (Fig. 1*B*). Starting from the human WT SOX/SOX homodimer, we first generated a SOX/Mo heterodimer with one fully functional SOX subunit and a truncated subunit lacking the N-terminal heme domain. This SOX/Mo

heterodimer has two active molybdenum centers but only one heme domain and serves as a control, given that heme activity cannot be assigned to either an intersubunit or an intrasubunit ET. The second heterodimer SOX/Mo_C264S consists of one fully functional FL SOX subunit and the heme-truncated subunit carrying the C264S substitution that abolishes sulfite oxidation at the molybdenum center. This restricts ET from molybdenum to heme to the functional FL SOX subunit. The third SOX_C264S/Mo heterodimer represents the reverse setting in which the active site C264S substitution abolishes sulfite reactivity of the FL subunit, which is, however, the only subunit harboring a heme domain. Hence, activity detected in this heterodimer would derive from electrons generated on a different Moco-active subunit.

Sequential affinity purification, utilizing first the N-terminal His-tag at one subunit followed by a second Strep-Tactin binding of a Strep-Tag at the N-terminus of the second subunit, allowed isolation of heterodimeric SOX variants that carried both affinity tags (Fig. 1*C*). Preparative size-exclusion chromatography (SEC) purified SOX dimers to homogeneity (Fig. 1*C*), whereas analytical SEC was used to reveal their heterodimeric state in solution (Fig. 1*D*). Here, heterodimeric SOX/Mo domain eluted with a calculated molecular weight of 105 kDa, which was in between the sizes of the SOX/SOX and Mo/Mo homodimers with calculated masses of 133 and 71 kDa, respectively (Fig. 1*D*). Purity of the proteins was confirmed by Coomassie brilliant blue staining of a 12% SDS gel, showing a band at approximately 60 and 50 kDa, representing the FL and heme-truncated subunit of SOX, respectively (Fig. 1*E*).

Distribution of Moco in SOX dimers

In order to ensure precise result interpretation, Moco saturations of the SOX/SOX, SOX/Mo, SOX/Mo_C264S, and SOX_C264S/Mo dimers were determined (28, 29). Given that the amount of Moco could only be determined per dimer, an additional activity determination of the Moco domains within a dimer was applied, by using the artificial electron acceptor hexacyanoferrate (ferricyanide [FeCN]). Note that FeCN accepts electrons solely from an active molybdenum site. We assumed a 50% decreased Moco-dependent FeCN activity of heterodimers in cases where one subunit harbors the C264S substitution. We found for the SOX/Mo heterodimer, 103.1 ± 18.5% of the FeCN-dependent activity per incorporated Moco, which is similar to the SOX/SOX homodimer (Fig. 2*A*). In contrast, the SOX/Mo_C264S and SOX_C264S/Mo heterodimers showed decreased FeCN reduction rate per incorporated Moco of 58.7 ± 14.7% and 58.6 ± 19.8% for SOX/Mo_C264S and SOX_C264S/Mo, respectively (Fig. 2*A*). This finding is consistent with a near equal Moco incorporation among both subunits of a given dimer, despite the presence of the C264S substitution (Fig. 2*A*).

Sulfite-dependent cytochrome c reduction by heterodimeric SOX variants

To monitor the complete catalytic cycle of SOX, the physiological electron acceptor cytochrome *c* was used in

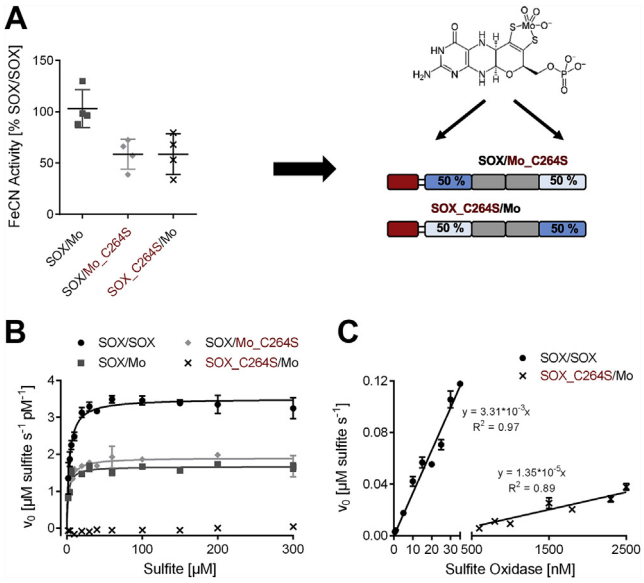

Figure 2. Steady-state kinetic analysis of heterodimeric SOX variants. *A*, comparison of k_{cat} values for the sulfite-dependent reduction of FeCN normalized to the activity of WT SOX/SOX. Moco is equally distributed between unmodified SOX and the subunit carrying the Cys264Ser substitution. *B* and *C*, steady-state sulfite-dependent reduction of cytochrome *c*. Reduction of cytochrome *c* was monitored at 550 nm in 100 mM Tris–Ac (pH 8.0). *B*, measurements were performed with 1 to 5 nM enzyme (based on Moco quantification), and varying sulfite concentrations were used. *C*, enzyme concentration-dependent steady-state cytochrome *c* reduction with sulfite excess (300 µM). FeCN, ferricyanide; Moco, molybdenum cofactor; SOX, sulfite oxidase; Tris–Ac, Tris(hydroxymethyl)aminomethane acetate salt.

sulfite-dependent steady state kinetics of the different SOX variants. Other than FeCN, cytochrome *c* accepts sulfite-derived electrons solely from the heme domain of SOX. Hence, IET within SOX is a prerequisite for steady-state cytochrome *c* reduction. We found both SOX variants that comprised at least one functional FL subunit displaying approximately 50% activity of the homodimeric WT control (Fig. 2*B* and Table 1). In contrast, cytochrome *c* reduction by heterodimeric SOX_C264S/Mo was strongly compromised. By increasing the SOX_C264S/Mo concentration, sulfite-dependent cytochrome *c* reduction was observed (Fig. 2*C*). This revealed an approximately 200-fold rate reduction in comparison to WT SOX/SOX (Fig. 2*C*). This indicates that IET within SOX occurs primarily within one subunit. The observed residual activity may be the result of either (i) an ET in *trans* within the same SOX heterodimer or (ii) electrons are passed from one heterodimer to the heme domain of another heterodimer *via* an intermolecular path.

Rapid reaction kinetics of heterodimeric SOX variants

In order to characterize the first ET in SOX, rapid enzyme kinetic measurements were performed using a stopped-flow instrument. Here, we recorded heme reduction rates upon ET from $Mo^{(IV)}$ to the heme iron using 5 µM protein and 300 µM sulfite, thus assuring pseudo–first order reaction kinetics. The reaction was monitored for 10 s and fitted (if not stated otherwise) with a triple-exponential curve with the rapid

Table 1
Summary of kinetic parameters

SOX variant	Cytochrome *c*[a]		Rapid reaction kinetics[b]			
	k_{cat} (s^{-1})	K_m (μM)	k_1 (s^{-1})	k_2 (s^{-1})	k_3 (s^{-1})	k_4 (s^{-1})
SOX/SOX	4.1 ± 0.6	3.5 ± 0.1	24.8 ± 2.0	2.09 ± 0.34	0.066 ± 0.020	0.017 ± 0.004
SOX/Mo	1.8 ± 0.4	2.3 ± 0.7	22.2 ± 2.5	1.82 ± 0.47	0.019 ± 0.005	0.0035 ± 0.0010
SOX/Mo_C264S	2.0 ± 0.6	2.5 ± 0.5	22.8 ± 4.2	2.23 ± 1.10	0.019 ± 0.003	0.0064 ± 0.0016
SOX_C264S/Mo	0.017 ± 0.003[c]	—	0.15 ± 0.06	0.0051 ± 0.0023		
Mo/Mo + R217W/R217W[d]			0.18 ± 0.07	0.0017 ± 0.0009		

[a] Reaction occurred at RT in 100 mM Tris–Ac (pH 8.0) with 120 μg porcine cytochrome *c*, 18.75 μg catalase, 1 to 5 nM active enzyme, and 2 to 300 μM sulfite.
[b] Reaction occurred at 10 °C in 50 mM Tris–Ac (pH 8.0) using 5 μM enzyme and 300 μM sulfite.
[c] Assay was modified, and 600 to 2500 nM enzyme were used with 300 μM sulfite, and the linear fit of velocity *versus* enzyme concentration was determined.
[d] For rapid kinetics, 2.5 μM Mo/Mo and 2.5 μM R217W/R217W were used.

k_1, occurring in about the first 0.1 s of the reaction, representing heme reduction upon the first IET from $Mo^{(IV)}$ (Fig. 3*A*). For homodimeric WT SOX/SOX, we recorded an IET rate (k_1) of 24.8 ± 2.0 s^{-1} (Fig. 3*D* and Table 1). Heterodimeric SOX/Mo and SOX/Mo_C264S were found to behave similarly (Fig. 3*D* and Table 1).

In contrast, and as expected from the steady-state kinetics, ET rates in the SOX_C264S/Mo heterodimer were significantly compromised. Instead of an initial rapid increase, representing an IET from $Mo^{(IV)}$ to heme, heme reduction showed a slow and gradual increase. Accordingly, the measurement period was extended to 300 s and fitted with a double exponential curve (Fig. 3*B*). Compared with the homodimeric WT SOX/SOX control, k_1 was approximately two orders of magnitude reduced (Fig. 3*D* and Table 1). The compromised heme reduction rate of SOX_C264S/Mo together with the unchanged rate of SOX/Mo_C264S implied that heme reduction preferentially occurs within one subunit. This indicates that the loss of this IET pathway predominantly accounts for the loss of activity seen in the sulfite:cytochrome *c* steady-state kinetics.

To determine whether residual SOX_C264S/Mo activity could be attributed to an ET between dimers, we first measured heme reduction of WT SOX/SOX using 5 μM enzyme and 300 μM sulfite for 300 s and fitted a quadruple exponential curve (Fig. 3*C*). The total absorption change of approximately 500 mAU was reached within 150 s with the initial rapid absorption change in the first 0.1 s accounting for a change of approximately 100 mAU. Given that only 35% of SOX/SOX homodimers and 15% of heterodimers in the

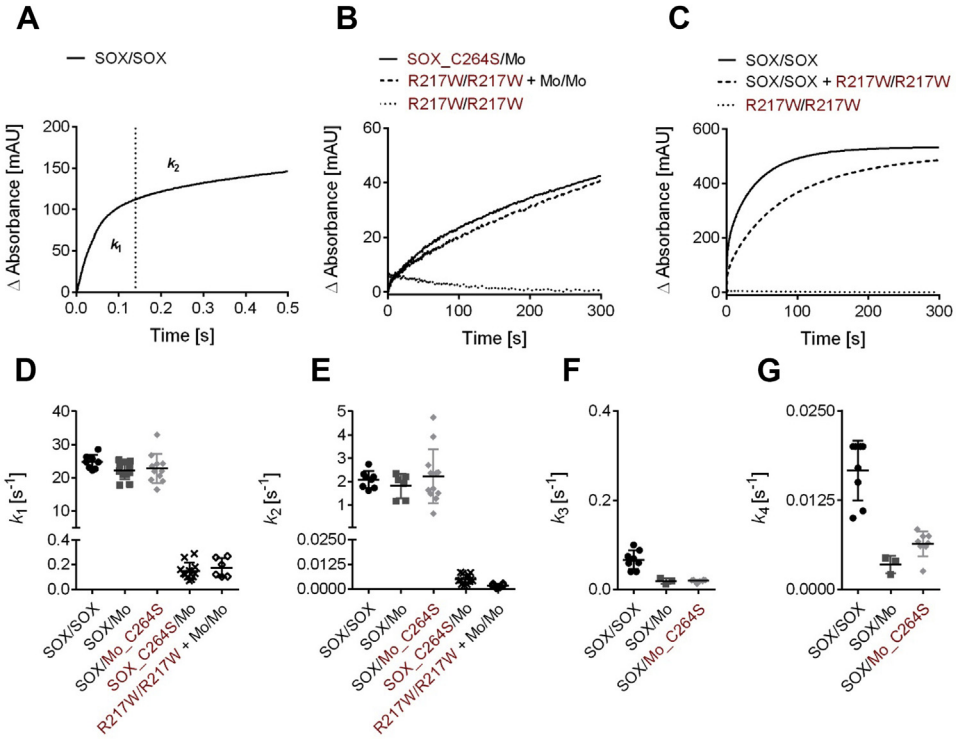

Figure 3. Rapid reaction kinetics of heterodimeric SOX. *A*, change in absorbance recorded for SOX/SOX during measurement with k_1 representing the initial rapid increase. Heme reduction was monitored at 423 nm at 10 °C in 50 mM Tris–Ac (pH 8.0) under anaerobic conditions with sulfite excess (300 μM). *B* and *C*, change in absorbance recorded at 423 nm over 300 s. In each experiment 5 μM enzyme was used except for the mix of R217W/R217W and Mo/Mo where 2.5 μM of each dimer was used. Kinetic traces in (*B*) and (*C*) were fitted with double and quadruple exponential curves, respectively. *D*–*G*, obtained values for k_1–k_4 derived from curve fittings in (*A*–*C*). SOX, sulfite oxidase; Tris–Ac, Tris(hydroxymethyl)aminomethane acetate salt.

reaction mixture contained Moco, it seems that the slower rates observed upon the initial fast rate represent reduction of heme cofactors in enzymes lacking Moco (Fig. 4*A*). This observation implies ET reactions beyond the traditional IET reaction within one subunit of SOX.

To probe intermolecular ET between different dimers, we expressed and purified the inactive SOX variant R217W as homodimeric enzyme (23). The absence of heme reduction in R217W/R217W was confirmed by rapid reaction kinetics (Fig. 3, *B* and *C*). As expected, when 2.5 μM SOX/SOX were mixed with 2.5 μM R217W/R217W and excess sulfite, the rate of intial heme reduction dropped by approximately 50% because of the replacement of 50% of the SOX by inactive R217W/R217W (Fig. 3*C*). However, following incubation time of 300 s, again nearly maximal heme reduction has been reached (Fig. 3*C*). This finding suggests that SOX/SOX can reduce the heme cofactors of R217W/R217W through interdimer ET.

Next, the experiment was repeated replacing SOX/SOX with homodimeric Mo/Mo lacking both heme domains. Since no heme reduction was recorded for R217W/R217W and Mo/Mo when present alone in the reaction, any heme reduction in a mixture of both must result from Moco-to-heme interdimer ET (Fig. 4*E*). Indeed, heme reduction was observed when R217W/R217W and Mo/Mo were both present in the reaction. Strikingly, the traces of heme reduction were remarkably similar to those recorded for SOX_C264S/Mo (Fig. 3*B*). This finding strongly indicates that in SOX_C264S/Mo, ET reactions to heme were also predominantly derived from interdimer reactions from Moco to heme (Fig. 4, *D* and *E*).

When comparing all determined ET rates in this study, one can conclude that the highly active variants (SOX/SOX, SOX/Mo, and SOX/Mo_C264S) share two fast rate constants (k_1 = 22.2–24.8 s^{-1} and k_2 = 1.8–2.2 s^{-1}), representing the first (from $Mo^{(IV)}$) and second (from $Mo^{(V)}$) IET within one subunit of the SOX dimer (Fig. 4, *A*–*C* and Table 1, see Discussion section).

The much lower rates that were only observed with very long incubation times (k_3 = 0.02–0.07 s^{-1} and k_4 = 0.003–0.02 s^{-1}) were similar to the compromised SOX_C264S/Mo variant and the mixture of R217W/R217W and Mo/Mo

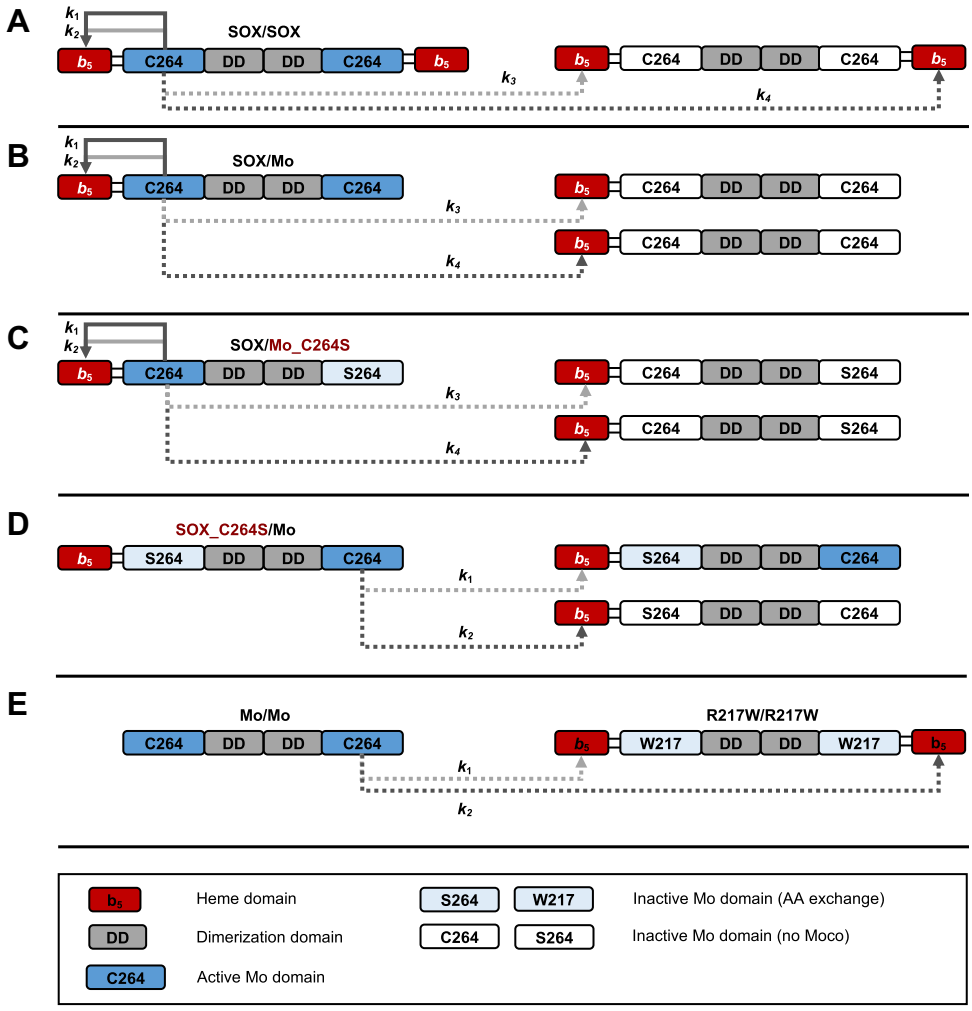

Figure 4. ET pathways in SOX. In a fully active and cofactor-saturated SOX subunit, IET occurs within one subunit. The IET from $Mo^{(IV)}$ and $Mo^{(V)}$ to heme in SOX/SOX (*A*), SOX/Mo (*B*), and SOX/Mo_C264S (*C*) is represented by k_1 and k_2. In SOX_C264S/Mo (*D*) and the R217W/R217W–Mo/Mo mix (*E*), no IET occurs. Here, k_1 and k_2 show the transfer of the $Mo^{(IV)}$ and $Mo^{(V)}$ electrons to heme *via* interdimer ET. Since the enzymes are not fully Moco saturated, these pathways also occur in *A*–*C*, giving rise to the detection of k_3 and k_4 values. ET, electron transfer; IET, intermolecular electron transfer; SOX, sulfite oxidase.

(Fig. 3, *D*–*G* and Table 1). Those rates can now be attributed to the first (from $Mo^{(IV)}$) and second (from $Mo^{(V)}$) intermolecular ET between different SOX dimers (Fig. 4, *D* and *E*). In expectation of interdimer third-order and fourth-order reaction kinetics, variations in k_3 and k_4 might be attributed to changes in availability of oxidized heme and/or Moco saturations that influence the ratio of available heme to Moco within the fast IET pathway.

Taken together, our results demonstrate that both the first and second IETs occur within one subunit of SOX, whereas electron bifurcation, which would involve ET from one subunit to another, can be excluded. Furthermore, we could dissect the complex network of ET in SOX, thereby shedding light onto the individual transfer rates under a single turnover condition of rapid reaction kinetics.

Discussion

SOX is a homodimeric molybdoheme enzyme. While the roles of the Moco and heme cofactors in detoxification of sulfite and regeneration of the enzyme are well understood, it has remained unclear what role dimerization may play in the catalytic cycle (14). Since four of 16 known missense mutations identified from ISOD patients localize to the dimerization domain, correct homodimerization appears to be key for SOX function (22). This is highlighted by a recent study that identified 15 novel ISOD-causing missense mutations of which another four localized to the dimerization domain (23). Given that the two metal atoms of the cofactors are too far apart in the crystal structure of chicken SOX to allow efficient IET (6, 18, 20), it is well accepted that a conformational change occurs, which is mediated by the flexible tether connecting the heme and Moco domain (16, 17). However, to date, the IET-competent conformation remains unknown. Thus, we asked the question whether SOX might adopt a conformation that allows IET between the molybdenum and iron atoms of opposing subunits. For the pathogenic G530D substitution in SOX, the monomeric state has been demonstrated *in vitro* (24, 25), and we asked the question whether pathogenicity may result from loss of electron bifurcation. This would not only account for the importance of homodimerization but also may explain the different rates observed for the first and second IET, respectively (18, 20).

The generation of heterodimeric SOX variants consisting of one WT and one truncated subunit allowed—based on our knowledge—for the first time the mechanistic separation of intrasubunit and intersubunit ET steps within the enzyme. By deleting the heme domain in one of the subunits and substituting the cysteine ligand of molybdenum for a serine residue (10) in one subunit, we created individual blocks in catalysis and ET in a given subunit. Previous reports show that the C264S variant retains the ability to bind Moco and to form homodimeric SOX (10), which has been confirmed by our study showing the formation of stable and isolatable SOX dimers with approximately 50% reduced sulfite-dependent FeCN activity.

Collectively, rapid reaction kinetic measurements and sulfite-dependent steady-state reduction of cytochrome *c* showed that both the first (k_1) and second IETs (k_2) occur within one subunit of SOX, given that the activity of SOX/Mo_C264S was comparable to SOX/Mo, whereas the activity of SOX_C264S/Mo was compromised by more than two orders of magnitude. Thus, our findings imply that one fully functional subunit is sufficient for catalytic activity, and the differences in rate determined for the first (k_1) and second IETs (k_2) are not attributed to electron bifurcation within an SOX dimer. The additional study of inactive SOX R217W/R217W with Mo/Mo demonstrated interdimer Mo-to-heme ET.

For SOX/SOX, a k_1 of 24.8 ± 2.0 s^{-1} was determined, which is similar to previously reported values (18, 19). Furthermore, a k_2 of 2.09 ± 0.34 s^{-1} was observed, which is faster than the intermolecular rates k_3 and k_4 (Fig. 3, *E*–*G*). Therefore, this observed k_2 value most likely represents the second intrasubunit IET from $Mo^{(V)}$ to heme in fully functional FL SOX (Fig. 4, *A*–*C*), requiring ET between individual heme molecules. Assuming that the liberation of such heme sites involves a much slower heme-to-heme ET, the lower rate for the electron derived from $Mo^{(V)}$ is not contradicting direct studies that have reported a much higher rate for the second ET (17, 20).

When comparing k_3 and k_4 of the active SOX variants to k_1 and k_2 of the compromised SOX_C264S/Mo variant, we conclude that the latter represent the slow rates of fully active enzyme and that the increased variability in their value may reflect changes in cofactor saturation. Because of the strict Moco-dependent maturation of SOX in mitochondria, all fully matured enzymes carry Moco *in vivo* (27, 28, 30). It is for this reason, that in mitochondria sulfite-derived electrons would predominantly follow intrasubunit IET. However, the ability of SOX to liberate electrons to other SOX molecules might potentiate its ability to use alternative electron acceptors, like nitrite, that are limited to the use of the $Mo^{(IV)}$ electron (18, 31–33).

We speculate that homodimerization in SOX is required for enhanced stability as a component of the maturation process rather than taking an active role in the overall SOX catalytic cycle (27). In conclusion, by generation of heterodimeric SOX variants, we were able to uncover that ET of SOX predominantly occurs within one subunit and that one fully functional subunit is sufficient for steady-state formation of sulfate from sulfite. Since SOX is the prototype for the family of Moco-containing enzymes, this study might provide insights into the mechanism of ET within other eukaryotic homodimeric molybdenum-dependent enzymes. For example, in the related plant nitrate reductase, each subunit of the homodimer carries a heme, a flavin adenine dinucleotide, and Moco. Therefore, we propose that in homodimeric Mo enzymes, ET occurs within one subunit.

Experimental procedures

Materials, plasmids, and bacterial strains

Oligonucleotides for PCR and sequencing were bought from Sigma–Aldrich. Restriction enzymes and T4 DNA ligase were

purchased from Thermo Scientific. The pQE-80L and petDUET-1 expression vectors were used and bought from Qiagen and Novagen, respectively. For protein expression, *Escherichia coli* TP1004 (ΔlacU169, araD139, rpsL150, relA1, flbB, deoC1, ptsF, rbsR, non-9, gyrA219, ΔmobAB) and TP1001 (F-[araD139]B/r Δ(argF-lac)169*&lambda-e14-flhD5301 Δ(fruK-yeiR)725 (fruA25)‡ relA1rpsL150(strR) rbsR22 Δ(fimB-fimE)632(::IS1) deoC1, ΔmobA) were used (34).

Cloning of heterodimeric SOX variants

Site-directed mutagenesis was used to generate the C264S substitution. Two PCR fragments, which harbored the mutation at the 3′ or 5′ end, were produced and subsequently fused by PCR. All inserts were amplified by PCR using primers designed to introduce restriction sites for the target multiple cloning site (MCS). The amplicon and plasmid were digested with restriction enzymes (Thermo Fisher Scientific) and ligated with T4 DNA ligase (Thermo Fisher Scientific) according to the manufacturer. The human Mo domain (A167–P545) and mature FL hSOX (E80–P545), both with and without the C264S substitution, were cloned into MCS1 and MCS2 of petDUET-1, respectively (6, 35). Mature FL hSOX was also cloned into pQE-80L. All constructs were sequenced (GATC Biotech AG) to confirm their identity.

Expression and purification of recombinant proteins

All proteins were expressed in LB media. The pQE-80L plasmid was expressed in TP1004 for 72 h at 18 °C, and the medium was supplemented with 250 μM IPTG and 1 mM sodium molybdate. The petDUET-1 plasmid was expressed in TP1001, the T7 RNA polymerase was stably integrated using the λDE3 lysogenization kit (Novagen), for 18 h at 30 °C, and the medium was supplemented with 25 μM IPTG and 0.5 mM sodium molybdate. Harvested cells were resuspended in lysis buffer (300 mM NaCl, 50 mM Tris(hydroxymethyl)aminomethane acetate salt [Tris–Ac] [pH 8.0]) and treated with lysozyme (VWR; 23,500 U/mg) for 30 min at RT. All further steps were carried out at 4 °C. Cells were disrupted with an Emulsiflex C-5 cell disruptor (Avestin). According to the protein tag, affinity chromatography using HIS-Select Nickel Affinity Gel (Sigma–Aldrich) and/or Strep-Tactin XT Superflow High Capacity resin (iba) was performed according to the manufacturer's instructions. For elution, 250 mM imidazole and 50 mM biotin in buffer W (1 mM EDTA, 150 mM NaCl, and 100 mM Tris/HCl [pH 7.5]) for elution, respectively. Proteins were further purified by SEC using a Superdex 200 column (120 ml; GE Healthcare) equilibrated with lysis buffer. For all proteins, buffer exchange to protein buffer (20 mM NaCl and 50 mM Tris–Ac [pH 8.0]) was performed using a PD10 column (GE Healthcare). The purity of the proteins was confirmed with 12% SDS-PAGE using Coomassie staining, and the dimerization state was confirmed using analytical SEC (Superdex 200, 25 ml; GE Healthcare). Mo domain and SOX R217W were expressed and purified as previously described (18, 23).

Determination of Moco saturation

The Moco saturation of recombinant proteins was determined as described previously (28, 29). Briefly, 100 pmol SOX were oxidized to FormA by overnight incubation with acidic Lugol's iodine solution in the dark. After precipitated protein was removed, fresh 1% ascorbic acid was added and buffered to pH 8.3 using Tris. Form A was dephosphorylated to dephospho-form A by treatment with alkaline phosphatase (Roche; 7500 U/ml) and 20 mM $MgCl_2$ for 30 min in the dark. The amount of dephospho FormA was determined with HPLC.

Sulfite:FeCN reduction

The reaction was carried out at RT in 200 μl 100 mM Tris–Ac (pH 8.0) with 268 μM potassium FeCN(III) (Sigma–Aldrich), 18.75 μg bovine catalase (Sigma–Aldrich), and 5 nM active enzyme. The change in absorption of FeCN upon addition of 300 μM sulfite was monitored at 420 nm with a TECAN Spark microplate reader. For all measurements, three technical replicates were performed and a negative control without enzyme. The initial velocity was calculated from the initial linear increase in absorption and the extinction coefficient of FeCN (1020 l mol^{-1} cm^{-1}).

Sulfite:cytochrome c reduction

Measurements were performed at RT in 200 μl 100 mM Tris–Ac (pH 8.0). The reaction consisted of 120 μg porcine cytochrome *c* (Serva), 18.75 μg bovine catalase (Sigma–Aldrich), 1 to 5 nM active enzyme, and 2 to 300 μM sulfite. Alternatively, 1 to 35 nM SOX/SOX or 600 to 2500 nM C264S/Mo were used with 300 μM sulfite. The absorption of cytochrome *c* was measured at 550 nm using a TECAN Spark microplate reader. Technical triplicates were measured along with one negative control without enzyme. The initial linear increase in absorption and the extinction coefficient of cytochrome *c* (19,630 l mol^{-1} cm^{-1}) were used to calculate the initial velocity.

Rapid reaction kinetics

Rapid reaction kinetics were measured anaerobically at 10 °C using an SX20 stopped-flow spectrometer (Applied Photophysics Ltd) as described by Kaczmarek *et al.* (18). Anaerobic conditions were insured through oxygen scavenging by incubating the device, syringes, and tubing for 1 h with 10 mM D-glucose, glucose oxidase (Sigma–Aldrich), and bovine catalase (Sigma–Aldrich) in 100 mM sodium acetate (pH 5.0). This was removed by washing with anaerobic assay buffer (50 mM Tris–Ac [pH 8.0]). Protein was thawed in a glove box (Coy laboratory products), and enzyme solutions were prepared using anaerobic assay buffer to give a final concentration of 5 μM. When a mix of two enzymes was measured, they were prepared to give a final concentration of 2.5 μM each. Sulfite solutions were prepared anaerobically in the same buffer to give a final concentration of 300 μM. The change in absorption of the cytochrome b_5 heme at 423 nm was monitored with a photon multiplier using a path length of 1 cm. Measurements

were performed as technical triplicates or quadruplicates. The data were fit as double, triple, or quadruple exponential curves with the Pro-Data SX software, which uses an iterative nonlinear least squares Levenberg–Marquardt algorithm.

Statistics

Two biological replicates were performed for WT SOX. For each heterodimeric SOX variant, three biological replicates were analyzed, except in sulfite:FeCN reduction. Here, only two biological replicates were analyzed, but the experiment was conducted twice. For kinetic curves, one representative dataset is shown. GraphPad Prism 6 (GraphPad Software, Inc) was used to create figures and calculate kinetic parameters.

Data availability

Experimental raw data are available to be shared upon request to the corresponding authors.

Acknowledgments—We thank Monika Laurien, Simona Jansen, Joana Stegemann, and Julia Reich for excellent technical assistance. We thank Laura Vierbaum for initiating the project. This research was funded by grant CMMC2017-C13 from the Center for Molecular Medicine Cologne, Germany.

Author contributions—G. S. and D. B. conceptualization; M. E. and A. T. K. methodology; M. E. validation; A. T. K. and D. B. formal analysis; M. E. and D. B. investigation; A. T. K. data curation; M. E. and A. T. K. writing–original draft; G. S. and D. B. writing–review & editing; M. E. visualization; A. T. K., G. S., and D. B. supervision; G. S. project administration; G. S. funding acquisition.

Conflict of interest—The authors declare that they have no conflicts of interest with the contents of this article.

Abbreviations—The abbreviations used are: ET, electron transfer; FeCN, ferricyanide; FL, full-length; hSOX, human SOX; IET, intramolecular electron transfer; ISOD, isolated SOX deficiency; MCS, multiple cloning site; Moco, molybdenum cofactor; SEC, size-exclusion chromatography; SOX, sulfite oxidase; Tris–Ac, Tris(hydroxymethyl)aminomethane acetate salt.

References

1. Cohen, H. J., Betcher-Lange, S., Kessler, D. L., and Rajagopalan, K. V. (1972) Hepatic sulfite oxidase. *J. Biol. Chem.* **247**, 7759–7766
2. Kumar, A., Dejanovic, B., Hetsch, F., Semtner, M., Fusca, D., Arjune, S., Santamaria-Araujo, J. A., Winkelmann, A., Ayton, S., Bush, A. I., Kloppenburg, P., Meier, J. C., Schwarz, G., and Belaidi, A. A. (2017) S-sulfocysteine/NMDA receptor–dependent signaling underlies neurodegeneration in molybdenum cofactor deficiency. *J. Clin. Invest.* **127**, 4365–4378
3. Edwards, M. C., Johnson, J. L., Marriage, B., Graf, T. N., Coyne, K. E., Rajagopalan, K. V., and MacDonald, I. M. (1999) Isolated sulfite oxidase deficiency: Review of two cases in one family. *Ophthalmology* **106**, 1957–1961
4. Ito, A. (1971) Hepatic sulfite oxidase identified as cytochrome b5-like pigment extractable from mitochondria by hypotonic treatment. *J. Biochem.* **1064**, 1061–1064
5. Schwarz, G., Mendel, R. R., and Ribbe, M. W. (2009) Molybdenum cofactors, enzymes and pathways. *Nature* **460**, 839–847
6. Kisker, C., Schindelin, H., Pacheco, A., Wehbi, W. A., Garrett, R. M., Rajagopalan, K. V., Enemark, J. H., and Rees, D. C. (1997) Molecular basis of sulfite oxidase deficiency from the structure of sulfite oxidase. *Cell* **91**, 973–983
7. Johnson, J. L., and Rajagopalan, K. V. (1977) Tryptic cleavage of rat liver sulfite oxidase. Isolation and characterization of molybdenum and heme domains. *J. Biol. Chem.* **252**, 2017–2025
8. Mendel, R. R. (2013) The molybdenum cofactor. *J. Biol. Chem.* **288**, 13165–13172
9. Rajagopalan, K. V., and Johnson, J. L. (1992) The pterin molybdenum cofactors. *J. Biol. Chem.* **267**, 10199–10202
10. Garrett, R. M., and Rajagopalan, K. V. (1996) Site-directed mutagenesis of recombinant sulfite oxidase: Identification of cysteine 207 as a ligand of molybdenum. *J. Biol. Chem.* **271**, 7387–7391
11. Peariso, K., McNaughton, R. L., and Kirk, M. L. (2002) Active-site stereochemical control of oxygen atom transfer reactivity in sulfite oxidase. *J. Am. Chem. Soc.* **124**, 9006–9007
12. Kappler, U., and Enemark, J. H. (2015) Sulfite-oxidizing enzymes. *J. Biol. Inorg. Chem.* **20**, 253–264
13. Hille, R. (1994) The reaction mechanism of oxomolybdenum enzymes. *Biochim. Biophys. Acta* **118**, 143–169
14. Feng, C., Tollin, G., and Enemark, J. H. (2007) Sulfite oxidizing enzymes. *Biochim. Biophys. Acta* **1774**, 527–539
15. Enemark, J. H., Astashkin, A. V., and Raitsimring, A. M. (2009) Structures and reaction pathways of the molybdenum centres of sulfite-oxidizing enzymes by pulsed EPR spectroscopy. *Biochem. Soc. Trans.* **36**, 1129–1133
16. Johnson-Winters, K., Nordstrom, A. R., Emesh, S., Astashkin, A. V., Rajapakshe, A., Berry, R. E., Tollin, G., and Enemark, J. H. (2010) Effects of interdomain tether length and flexibility on the kinetics of intramolecular electron transfer in human sulfite oxidase. *Biochemistry* **49**, 1290–1296
17. Feng, C., Kedia, R. V., Hazzard, J. T., Hurley, J. K., Tollin, G., and Enemark, J. H. (2002) Effect of solution viscosity on intramolecular electron transfer in sulfite oxidase. *Biochemistry* **41**, 5816–5821
18. Kaczmarek, A. T., Strampraad, M. J. F., Hagedoorn, P. L., and Schwarz, G. (2019) Reciprocal regulation of sulfite oxidation and nitrite reduction by mitochondrial sulfite oxidase. *Nitric Oxide* **89**, 22–31
19. Wilson, H. L., and Rajagopalan, K. V. (2004) The role of tyrosine 343 in substrate binding and catalysis by human sulfite oxidase. *J. Biol. Chem.* **279**, 15105–15113
20. Pacheco, A., Hazzard, J. T., Tollin, G., and Enemark, J. H. (1999) The pH dependence of intramolecular electron transfer rates in sulfite oxidase at high and low anion concentrations. *J. Biol. Inorg. Chem.* **4**, 390–401
21. Schwarz, G. (2005) Molybdenum cofactor biosynthesis and deficiency. *Cell. Mol. Life Sci.* **69**, 2792–2810
22. Claerhout, H., Witters, P., Régal, L., Jansen, K., Van Hoestenberghe, M. R., Breckpot, J., and Vermeersch, P. (2018) Isolated sulfite oxidase deficiency. *J. Inherit. Metab. Dis.* **41**, 101–108
23. Kaczmarek, A. T., Bahlmann, N., Thaqi, B., May, P., and Schwarz, G. (2021) Machine learning-based identification and characterization of 15 novel pathogenic SUOX missense mutations. *Mol. Genet. Metab.* **134**, 188–194
24. Wilson, H. L., Wilkinson, S. R., and Rajagopalan, K. V. (2006) The G473D mutation impairs dimerization and catalysis in human sulfite oxidase. *Biochemistry* **45**, 2149–2160
25. Feng, C., Wilson, H. L., Tollin, G., Astashkin, A. V., Hazzard, J. T., Rajagopalan, K. V., and Enemark, J. H. (2005) The pathogenic human sulfite oxidase mutants G473D and A208D are defective in intramolecular electron transfer. *Biochemistry* **44**, 13734–13743
26. Tejada-Jimenez, M., Chamizo-Ampudia, A., Calatrava, V., Galvan, A., Fernandez, E., and Llamas, A. (2018) From the eukaryotic molybdenum cofactor biosynthesis to the moonlighting enzyme MARC. *Molecules* **23**, 3287
27. Klein, J. M., and Schwarz, G. (2012) Cofactor-dependent maturation of mammalian sulfite oxidase links two mitochondrial import pathways. *J. Cell Sci.* **125**, 4876–4885
28. Bender, D., Kaczmarek, A. T., Santamaria-Araujo, J. A., Stueve, B., Waltz, S., Bartsch, D., Kurian, L., Cirak, S., and Schwarz, G. (2019) Impaired

mitochondrial maturation of sulfite oxidase in a patient with severe sulfite oxidase deficiency. *Hum. Mol. Genet.* **28**, 2885–2899

29. Johnson, J. L., Hainline, B. E., Rajagopalan, K. V., and Arison, B. H. (1984) The pterin component of the molybdenum factor. Structural characterization of two fluorescent derivatives. *J. Biol. Chem.* **259**, 5414–5422
30. Kaczmarek, A. T., Bender, D., Gehling, T., Kohl, J. B., Daimagüler, H. S., Santamaria-Araujo, J. A., Liebau, M. C., Koy, A., Cirak, S., and Schwarz, G. (2021) A defect in molybdenum cofactor binding causes an attenuated form of sulfite oxidase deficiency. *J. Inherit. Metab. Dis.* https://doi.org/10.1002/jimd.12454
31. Bender, D., Kaczmarek, A. T., Kuester, S., Burlina, A. B., and Schwarz, G. (2020) Oxygen and nitrite reduction by heme-deficient sulphite oxidase in a patient with mild sulphite oxidase deficiency. *J. Inherit. Metab. Dis.* **43**, 748–757
32. Bender, D., Kaczmarek, A. T., Niks, D., Hille, R., and Schwarz, G. (2019) Mechanism of nitrite-dependent NO synthesis by human sulfite oxidase. *Biochem. J.* **476**, 1805–1815
33. Wang, J., Krizowski, S., Fischer-Schrader, K., Niks, D., Tejero, J., Sparacino-Watkins, C., Wang, L., Ragireddy, V., Frizzell, S., Kelley, E. E., Zhang, Y., Basu, P., Hille, R., Schwarz, G., and Gladwin, M. T. (2015) Sulfite oxidase catalyzes single-electron transfer at molybdenum domain to reduce nitrite to nitric oxide. *Antioxid. Redox Signal.* **23**, 283–294
34. Palmer, T., Santini, C. L., Iobbi-Nivol, C., Eaves, D. J., Boxer, D. H., and Giordano, G. (1996) Involvement of the narJ and mob gene products in distinct steps in the biosynthesis of the molybdoenzyme nitrate reductase in Escherichia coli. *Mol. Microbiol.* **20**, 875–884
35. Ono, H., and Ito, A. (1984) Transport of the precursor for sulfite oxidase into intermembrane space of liver mitochondria: Characterization of import and processing activities. *J. Biochem.* **95**, 345–352